UT TENSIO SIC VIS

SERVICES DE LA RECHERCHE

Rapport technique EP 81-R-4
Classification: Library of Congress No ...

A NUMERICAL STUDY ON NATURAL CONVECTION HEAT TRANSFER WITH DENSITY INVERSION OF WATER WITHIN A HORIZONTAL CYLINDRICAL ANNULUS

by

P. VASSEUR, L. ROBILLARD and B. CHANDRA SHEKAR

January 1981

Ecole Polytechnique de Montréal

Campus de l'Université
de Montréal
Case postale 6079
Succursale 'A'
Montréal, Québec
H3C 3A7

Rapport technique EP 81-R-4
Classification: Library of Congress No ...

A NUMERICAL STUDY ON NATURAL CONVECTION HEAT TRANSFER WITH DENSITY INVERSION OF WATER WITHIN A HORIZONTAL CYLINDRICAL ANNULUS

by

P. VASSEUR, L. ROBILLARD and B. CHANDRA SHEKAR

January 1981

A NUMERICAL STUDY ON NATURAL CONVECTION HEAT TRANSFER WITH DENSITY INVERSION OF WATER WITHIN A HORIZONTAL CYLINDRICAL ANNULUS

By

P. VASSEUR, L. ROBILLARD and B. CHANDRA SHEKAR

Department of Civil Engineering
Ecole Polytechnique, Université de Montréal
C.P. 6079, Succursale "A", Montréal, Canada - H3C 3A7

ABSTRACT

The effect of density inversion on steady natural convection heat transfer of cold water between two horizontal concentric cylinders is studied numerically. Water near its freezing point is characterized by a density maximum at $4^{o}C$. Numerical solutions are obtained for cylinders with size parameter A ranging from 2.2×10^{6} to 4.3×10^{9}, gap ratio B from 0.11 to 0.8. The temperature of the inner cylinder is maintained at $T_i = 0^{o}C$ while temperatures of the outer cylinder T_o are varied from 2 to $12^{o}C$. The results obtained are presented graphically in the form of streamline and isotherm contour plots. The heat transfer characteristics, velocity profiles and local and global Nusselt numbers are studied. The results of the present study were found qualitatively valid when compared with an experimental investigation carried out in the past.

NOMENCLATURE

A	size parameter gL^3/α^2
B	gap ratio $(L/2r_i)$
L	gap width $(r_o - r_i)$
Nu	local Nusselt number
$\overline{Nu}$	average Nusselt number
Nu_G	global Nusselt number
Pr	Prandtl number ν/α
r	radial coordinate
Δr	radial spacing between gridlines
R	dimensionless radial coordinate
R_L	dimensionless radius $(r - r_i)/(r_o - r_i)$
R_{AL}	Rayleigh number based on gap width $\frac{g\beta(\Delta T)(L)^3}{\nu\alpha}$
T	water temperature
ΔT	$T_o - T_i$
T_o	temperature of outer cylinder
T_i	temperature of inner cylinder
t	time
u,v	radial and angular velocities
U,V	dimensionless radial and angular velocities

Greek Symbols

Φ	angular coordinate
$\Delta\Phi$	angular spacing between gridlines
ω	vorticity
Ω	dimensionless vorticity
ψ	stream function
Ψ	dimensionless stream function
α	thermal diffusivity
β	thermal coefficient of volumetric expansion
ν	kinematic viscosity
μ	dynamic viscosity
$\beta_1 \ldots \beta_4$	constants (see equation (7))
ρ	water density
$\Delta\overline{\rho}$	$(\overline{\rho} - \rho(\Theta))/\overline{\rho}$
Θ	dimensionless temperature
τ	dimensionless time

SUPERSCRIPTS

-	refers to average value

SUBSCRIPTS

i	refers to inside cylinder
o	refers to outside cylinder

1 - INTRODUCTION

The steady laminar natural convection in a horizontal concentric cylindrical annulus has been studied in the past both analytically and experimentally [1-3]. In all those investigations, a linear relation between fluid density and its temperature has been assumed, such an assumption being acceptable for most fluids. However, in the case of water near its freezing point a linear relationship is not justified. In fact, the density of water reaches a maximum value at 3.98°C, thereafter decreasing with decreasing temperature. It results from this nonlinearity that convective motion in water behaves in a rather peculiar manner when the temperature domain encompasses the 3.98°C point, for the density of water is maximum at this temperature [4]. Since the pioneering works of Ede [5] and Merk [6], the problem of buoyancy induced flows in cold water has been studied by many investigators, not only because of their intriguing features but also due to the fact that they are a very common occurence in our environment and in many processes in technology.

The behaviour of convective motion of enclosed water, in the region of maximum density, has been studied in the past for several different geometries, boundary conditions, and temperature gradients. For instance Desai & Forbes [7] and Watson [8] have investigated numerically the heat transfer and flow patterns in cold water in a rectangular enclosure with vertical boundaries maintained at different temperatures and insulated horizontal boundaries. Similarly, the effect of density inversion on

natural convection heat transfer of a melted water contained in two horizontal concentric cylinders whose surface temperatures are kept isothermal has been studied experimentally by Seki et al [9]. It was found that, under certain conditions the flow was bicellular, in contrast to the one cell flow obtained for a fluid without maximum density effect, and as a result the heat transfer occurred primarily by conduction.

The transient behaviour of water, contained in a rigid rectangular insulator and cooled from above to near freezing has been considered by Forbes & Cooper [10]. Vasseur and Robillard [11] have studied the transient cooling of water, enclosed in a rectangular cavity with wall temperature maintained at $0^{o}C$. Supercooling of water contained in an enclosure subjected to convective boundary condition has been investigated by Cheng & Takeuchi [12] and Robillard & Vasseur [13] for the case of a circular pipe and a rectangular cavity, respectively. All these studies indicate that the resulting flow motion is greatly influenced by the presence of a maximum density effect, which drives the initial circulation inside the cavity and subsequently reverses it. The resulting heat transfer is thus reduced in comparison to a standard situation without maximum density effect.

The purpose of this investigation is to study analytically the effect of density inversion on the free convective heat transfer of a mass of water contained in a horizontal cylindrical annulus whose surface temperatures are kept isothermal. The present study is an extension of the experimental work of Seki et al [9]. Numerical studies of natural convection inside two horizontal concentric cylinders, in

the absence of maximum density effect, have been carried out in the past by many investigators; that of Kuehn & Goldstein [3] contains a comprehensive bibliography.

2 - PROBLEM FORMULATION

The problem under consideration is that of two-dimensional laminar convection of a mass of cold water enclosed between two horizontal concentric cylinders (see Fig. 1). It is assumed that the temperature of each cylinder is uniform, the inner cylinder being colder. Utilizing cylindrical coordinates, let the angular coordinate Φ be measured from the upward vertical line, $\Phi = 0$. The flow is symmetrical about a vertical plane through the axis of the cylinder. Accordingly, attention is confined to the range $0 \leqslant \Phi \leqslant \pi$. All fluid properties, except the water density, are taken to be constant and evaluated at the arithmetic mean temperature of the two cylinders.

The governing equations for the present problem, using the Oberbeck-Boussinesq approximation [14,15] and neglecting viscous dissipation and compressibility effects, are then given in nondimensional form as:

$$\frac{\partial \Omega}{\partial \tau} + \frac{1}{R}\left[\frac{\partial}{\partial R}(UR\Omega) + \frac{\partial}{\partial \Phi}(\Omega V)\right] = Pr\ \nabla^2\Omega + A\left[\sin\Phi\ \frac{\partial}{\partial R}\overline{\Delta\rho} + \frac{\cos\Phi}{R}\cdot\frac{\partial}{\partial \Phi}\overline{\Delta\rho}\right] \qquad [1]$$

$$\frac{\partial \Theta}{\partial \tau} + \frac{1}{R}\left[\frac{\partial UR\Theta}{\partial R} + \frac{\partial V\Theta}{\partial \Phi}\right] = \nabla^2\Theta \qquad [2]$$

$$\Omega = -\nabla^2\Psi \qquad [3]$$

$$U = \frac{1}{R}\frac{\partial\Psi}{\partial\Phi} \qquad V = -\frac{\partial\Psi}{\partial R} \qquad [4]$$

where

$$\tau = \frac{\alpha t}{L^2} \qquad U = \frac{uL}{\alpha} \qquad V = \frac{vL}{\alpha}$$

$$\Theta = \frac{T - T_i}{\Delta T} \qquad \Delta T = T_o - T_i \qquad R = \frac{r}{L}$$

$$\Psi = \frac{\psi}{\alpha} \qquad \Omega = \frac{\omega L^2}{\alpha} \qquad \overline{\Delta\rho} = \frac{\overline{\rho} - \rho(\Theta)}{\overline{\rho}}$$

$$\nabla^2 = \frac{\partial}{\partial R^2} + \frac{1}{R}\frac{\partial}{\partial R} + \frac{1}{R^2}\frac{\partial^2}{\partial\Phi^2} \qquad [5]$$

$$Pr = \nu/\alpha \qquad A = gL^3/\alpha^2$$

$$L = r_o - r_i \qquad B = L/2r_i$$

and all other symbols are defined in Nomenclature.

The initial and boundary conditions are:

$$U = V = \Psi = \Omega = 0;\ \Theta = 0 \quad \text{at } \tau = 0$$

$$U = V = \Psi = 0\ ;\ \Theta = 0 \quad \text{on the inner cylinder}$$

$$U = V = \Psi = 0\ ;\ \Theta = 1 \quad \text{on the outer cylinder} \qquad [6]$$

$$\frac{\partial U}{\partial\Phi} = V = \Psi = \Omega = 0;\ \frac{\partial\Theta}{\partial\Phi} = 0 \quad \text{at } \Phi = 0, \pi \text{ (symmetry lines)}$$

It is observed in the boundary conditions that use has been made of the symmetry of the problem with respect to a vertical plane passing through the axis of the cylinder. In fact, even if secondary flows

exist they must necessarily appear as counterrotating eddies symmetrically located.

When considering the temperature range $0 \sim 20^{o}C$ [16], the density-temperature relationship of water can be approximated by the following equation with an error of less than one unit at the last digit of the tabulated data of Landolt-Börnstein [17]:

$$\frac{\rho_o}{\rho} = 1 + \beta_1 T + \beta_2 T^2 + \beta_3 T^3 + \beta_4 T^4 \qquad [7]$$

where: $\rho_o = 0.9998396$ (g cm^{-3});

$\beta_1 = -0.678964520 \times 10^{-4} (1/^{o}C)$;

$\beta_2 = 0.907294338 \times 10^{-5} (1/^{o}C^2)$;

$\beta_3 = -0.964568125 \times 10^{-7} (1/^{o}C^3)$;

$\beta_4 = 0.873702983 \times 10^{-9} (1/^{o}C^4)$;

Local Nusselt numbers, representing the ratio of the effective thermal conductivity to the actual thermal conductivity, are defined for the inner and outer cylinder surfaces respectively by:

$$Nu_i = \frac{2r_i}{L} \left.\frac{\partial \Theta}{\partial R}\right|_i \qquad [8]$$

and

$$Nu_o = \frac{2r_o}{L} \left.\frac{\partial \Theta}{\partial R}\right| \qquad [9]$$

Mean or average values of the Nusselt number at each surface are then given by:

$$\overline{Nu}_i = \frac{2r_i}{\pi L} \int_0^{\pi} \left.\frac{\partial \Theta}{\partial R}\right|_i d\Phi \qquad [10]$$

and

$$\overline{Nu}_o = \frac{2r_o}{\pi L} \int_0^{\pi} \left.\frac{\partial \Theta}{\partial r}\right|_o d\Phi \qquad [11]$$

An energy balance for the inner and outer cylinder shows that the values of $\overline{Nu}_i$ and $\overline{Nu}_o$ should be equal. However, since the equations [10] and [11] were integrated numerically using Simpsons rule, the obtained values of $\overline{Nu}_o$ and $\overline{Nu}_i$ differed by about 1%. Thus, a global Nusselt number Nu_G was defined simply as the arithmetic mean of $\overline{Nu}_i$ and $\overline{Nu}_o$.

3 - NUMERICAL SOLUTION OF THE GOVERNING EQUATIONS

The coupled transport and energy equations (1) and (2) are quasi-linear, second-order partial differential equations of the parabolic type and such numerical methods as standard explicit method, alterning direction implicit method, Dufort-Frankel method and others may be applicable. In this study a two-dimensional alternating direction (A.D.I.) procedure is employed and the computational method involved differs slightly from that used by Mallison and de Vahl Davis [18]. The first and second derivative were approximated by central differences and the time derivatives by a first order forward difference. The finite difference forms of the equations were written in conservative form for the advective terms in order to preserve the transportive property [19]. The A.D.I. technique has the

advantage over explicit methods that it is numerically more stable and hence allows the use of a larger time step $\Delta\tau$. However, it has the disadvantage that each iteration requires more computations than does an iteration with the explicit techniques.

The elliptic equation for the stream function, equation (3), was solved by the method of successive over-relaxation (S.O.R.) for the new field which is then used to obtain the velocities from equation (4) and the wall vorticity (which requires the velocity boundary conditions). The major disadvantage of the S.O.R. method is the task of choosing the optimum relaxation coefficient for a given situation. For the present problem it was found that a relaxation factor of 1.8 was an optimum value and the iterative procedure was repeated until the following condition was satisfied:

$$\text{Max} \left| \frac{\psi^{n+1}_{i,j} - \psi^{n}_{i,j}}{\psi^{n+1}_{i,j}} \right| \leqslant 0.5 \times 10^{-3}$$

where the subscripts (n) and (n+1) indicates the values of the n^{th} and $(n+1)^{th}$ iterations, respectively. A useful method for checking the convergence of the steady state solution was to compare the average Nusselt number for the inner and outer cylinder.

Several different mesh sizes have been used, the choice depending largely on the size of the cavity. The mesh size in the r-direction ranged from $\Delta r = 1/18$ to $1/30$. In the Φ-direction a mesh size of $\Delta\Phi = \pi/18$ to $\pi/30$ was chosen. Typical values of the time step were 0.0001 and 0.0005. The total time steps ranged from 1600 to 2500 and

the corresponding computing time was from 530 to 680 s. on the IBM 360/70 computer.

To expedite plotting of the results, an auxilliary computer program was developed to locate points lying on specified isotherms and streamlines by linear interpolation of the computed values at the grid points. All graphs were performed using CALCOMP 563 automatic plotter.

4 - RESULTS AND DISCUSSION

In view of the number of parameters involved in the present problem, namely A, B, T_o and T_i numerical solutions are presented only for typical cases. It is worthwhile to notice that assuming a second order instead of a fourth order polynomial in equation (7) would make it possible to reduce by one the number of parameters involved in the present problem. However, this procedure would be done at the expense of a certain precision in the computation.

In order to verify the consistency of the present numerical study, the first cases considered were those corresponding to already published results on fluids with linear temperature - density relationship. Results for some of the cases studied by Crawford & Lemlich [20] and Kuehn & Goldstein [3] for various radius ratios r_o/r_i, Prandtl numbers Pr and Rayleigh numbers R_{AL} were obtained. The current analysis predicted essentially identical results for the flow patterns, temperature profiles and overall equivalent conductivity. For instance, for $R_{AL} = 8.925 \times 10^3$, Pr = 0.714 and B = 0.5 an equivalent conductivity of 1.749 was obtained

in the present investigation as compared with the values of 1.765 and 1.792 reported respectively by the two previous studies. An analytical result with $R_{AL} = 1.842 \times 10^3$, Pr = 0.7 and B = 0.425 presented by Mack & Bishop [2] was also checked. Again very close agreement was found between their results and those of the present analysis. However, the values of local Nusselt numbers were not in good agreement near $\Phi = 0$ and π positions, where deviations of about 12 per cent occurred. This point has also been observed by Powe and al [1] and may be due to the slow convergence of the power series used by Mack & Bishop. Having thus gained confidence in the present numerical analysis, attemps were done to predict the effects of density inversion on steady natural convection heat transfer of water between two horizontal concentric cylinders. The results obtained will be now discussed in the following sections.

Flow and isotherm patterns: Figs. 2 to 5 show typical results obtained for annuli with size parameter $A = 2.2 \times 10^9$, gap ratio B = 0.8, inside cylinder temperature $T_i = 0^oC$ and for different outside cylinder temperatures T_o varying between 4^oC and 12^oC. The corresponding dimensionless angular velocity V at $\Phi = 90^o$ as a function of dimensionless radius R_L is presented in Fig. 6. As mentioned earlier the problem under consideration is symmetrical with respect to a vertical axis and it was found advantageous to reproduce computer results on a single graph with the flow pattern on the right half of the cavity and the isotherms on the left half.

Fig. 2 shows the flow and isotherm patterns obtained for $T_o = 4^oC$. The fluid near the outer cylinder being at 4^oC is heavier and is moving downward while the relatively lighter fluid near the inner cylinder is moving upward. As a consequence of the symmetry and the continuity, the resulting fluid motion inside the whole cavity consists of two counterrotating vortices. Fig. 1 only shows the right clockwise vortex. The resulting velocity profile at $\Phi = 90^o$ is given in Fig. 6. The distortion of isotherms in Fig. 2 indicates a strong convective motion inside the cavity. It is also noticed that the maximum heat transfer, indicated by closely spaced isotherms, is located at the top of the cavity for the outer cylinder and at its bottom for the inner one. Since in the present case the outer wall temperature corresponds exactly to the maximum water density, no inversion effects are present. In fact, the flow pattern depicted in Fig. 2 is similar in form to the two usual thermoconvective cells, symmetrical with respect to the vertical axis, that have been described extensively in literature [3, 20, 21] for the case of an ordinary fluid.

Fig. 3 shows the flow pattern obtained for $T_o = 6.5^oC$ and it is seen that the flow field is now characterized by the presence of two counterrotating circulations of approximately equal size as indicated by the dividing streamline. This particular streamline corresponds to the value $\Psi = 0$ of the boundary and is left unconnected with it by the auxiliary computer program used to plot the graphs. The present flow pattern is a direct consequence of the maximum density of water at 4^oC. The heavy

dashed line represents the $4^{o}C$ isotherm and thus defines the region of maximum density. The fluid in the neighborhood of this line is heavier and, as a result moves downwards. On the boundaries, the fluid is lighter and moves upwards. The distortion of the isotherm patterns in the upper part of the cavity is a result of the intense convective motion generated by the clockwise vortex located in this region.

Fig. 4 shows that for $T_o = 8^{o}C$ two eddies are still present inside the cavity as in the case of Fig. 3. However, it can be noticed that the eddy near the outer cylinder is now larger, while the one near the inner cylinder is smaller. Further, it is seen from the isotherm field that the convective motion inside the cavity is still considerably reduced as compared with the case with $T_o = 4^{o}C$. For outside cylinder temperature of $12^{o}C$, Fig. 5 shows that the inner cell has completely disappeared and the circulation is now counterclockwise. Furthermore, the local heat transfer in the present case is now maximum at the bottom of the outer cylinder and at the top of the inner one. This situation is completely opposite to the case described in Fig. 2. In Fig. 6 a comparison between the velocity profiles for $T_o = 4^{o}C$ and $T_o = 12^{o}C$ illustrates the opposite behaviour.

The flow and isotherm patterns of Fig. 7 for $T_o = 4^{o}C$, $B = 0.11$, and $\frac{r_o}{r_i} = 1.215$ are considerably different from those obtained in Fig. 2. Thus, in the wider gap the flow has the kidney shape described by Bishop and Carley [22]. In the present case the flow, due to the narrower gap

involved, has rather the crescent shape also described by Bishop and Carley. Furthermore, the isotherms depicted in Fig. 6 appear to be very similar to those which would occur in the case of pure conduction, i.e. they are almost concentric circles. This is due to the small gap ratio involved in this case. However, a non negligible convective motion is revealed by the spacing between the isotherms which varies strongly with position.

An experimental study on natural convection heat transfer with density inversion of water between two horizontal concentric cylinders has been conducted in the past by Seki et al [9]. The experimental model consisted of concentric cylinders with radius ratio ranging from 1.18 to 6.39. Temperature of the inner cylinder was maintained at $0^{o}C$, while temperature of the outer cylinder was varied from 1 to $15^{o}C$, with Grashof number $G_r = g\beta\Delta T\, L^3/\nu^2$ ranging from 3.2×10^1 to 2.7×10^5. Photographs and qualitative description of the flow patterns, temperature profiles, local and average Nusselt number were presented. The present numerical method could not simulate adequately the high convective motion involved in most of Seki's experimental results. Nevertheless, a similar trend was observed in many aspects. For instance, the sequence of events appearing in Figs. 2 to 5, i.e. formation of unicellular clockwise and anticlockwise vortices or bicellular flow depending on the temperature T_c, were comparable.

It has been possible to verify one of the cases studied by Seki which involves relatively low convection. A similar flow pattern was obtained numerically and is shown in Fig. 6. However, Seki et al have observed the formation of a very small counterclockwise eddy at the top of their cavity. This secondary eddy, that was attributed to the effects of the

gap width and cylinder curvature, could not be reproduced by the numerical solution of the present study. This is probably due to the fact that, in order to generate this secondary eddy by numerical method, an initial disturbance should have been introduced in the flow field.

Another interesting result of the present study is the tendency for the clockwise circulation pattern to form two cells. This phenomenon, shown in Fig. 3, was observed to occur only for a limited temperature range between $T_o = 6.5^oC$ to 7.25^oC. A similar vortex formation has been reported by Saitoh and Hirose [23] in their study of the convection flow surrounding an horizontal ice cylinder. Their experimental observations have revealed the existence of an additional vortex pair over the ice cylinder. Such a phenomenon was observed for a temperature range between 5.5 and 6.5^oC.

Temperature Distributions and Nusselt Numbers

Figs. 8(a) and 9(a) show typical dimensionless temperature Θ as a function of dimensionless radius R_L. The corresponding local Nusselt numbers based on inner and outer cylinder, as defined in equations (8) and (9), are shown in Figs. 8(b) and 9(b). In these figures the pure conduction curves and the 4^oC isotherms, when they exist, are represented by broken lines.

Fig. 8(a) shows Θ versus R_L for the case with $T_o = 4^oC$. As already mentioned this case corresponds to the presence of a single clockwise circulation in the right half cavity. In the thermal boundary layer adjacent to the outer cylinder it is seen that the temperature gradient

increases considerably as the angular position decreases from $\Phi = 180^{o}$ towards $\Phi = 0^{o}$. However, it is observed that near the inner cylinder the trend is opposite. A temperature reversal in the central portion of the gap, for Φ ranging from 0^{o} and 90^{o}, may also be observed. This is probably due to higher heat transport by angular convection flow rather than radial one. The corresponding local Nusselt for this case is shown in Fig. 8(b). In agreement with the aforementioned behaviour of the temperature profile, the Nusselt number reaches the minimum value at 180^{o} on the outer cylinder and 0^{o} on the inner one. Naturally the results obtained for $T_{o} = 12^{o}C$ were found to have opposite tendency.

The results for $T_{o} = 6.5^{o}C$ are presented in Fig. 9(a). It is noted that, except for the angular position $\Phi = 0^{o}$, the temperature profiles inside the cavity follow approximately the trend given by the pure conduction curve. This is due to the fact that inside the cavity two eddies of almost equal size coexist. The intense convection indicated by the temperature curve at $\Phi = 0^{o}$ results from the presence of the secondary clockwise circulation in this region. The behaviour of the Nusselt number is depicted in Fig. 9(b) and it is seen that at the top of the cavity the Nusselt number is maximum on the outer cylinder and minimum on the inner one. The influence of the flow circulation in the upper region of the annulus on the inner cylinder is seen to be important. Thus, the Nusselt number passes through a peak value at $\Phi = 20^{o}$ and a minimum, close to the pure conduction value, at $\Phi = 50^{o}$, thereafter increasing with increasing angular position.

Fig. 10 shows the relation between the average Nusselt number Nu_G and ΔT ($=T_o$) the temperature difference between the outer and inner cylinder. This figure reveals that Nu_G does not increase monotonously from pure conduction value (2.09) at $T_o = 0^oC$ with increasing ΔT as on common fluids having a linear density-temperature relationship. In fact, Nu_G increases monotonously as T_o becomes higher only when a single large eddy occupies the major portion of the gap as in the case $T_o \leqslant 4^oC$ or $T_o \geqslant 10^oC$. After reaching the peak value at 4^oC a minimum value of Nu_G is observed at about $T_o \simeq 7^oC$. This temperature corresponds to a situation in which two vortices of approximately equal strength exist in the gap. Under this circumstance the fluid velocities are small and the convective heat transfer mechanism reaches its minimum efficiency. Furthermore it is observed that an increase of L correspond in an increase of convective motion and consequently an increase of Nu_G. It is worth while to mention at this stage that a minimum average Nusselt number has also been observed in the past for the case of natural convection heat transfer under the influence of density inversion in a rectangular cavity. Analytical studies reported by Watson [8] and Robillard & Vasseur [24] have shown that for this type of geometrical configuration a minimum value of the average Nusselt number occurs at 8^oC. The temperature at which the minimum Nu_G occurs is less in the case of cylindrical annuli compared to that of rectangular cavity. This may be due to the fact that for an annulus the heat area of the outer cylinder is larger than cooling area of the inner cylinder.

5 - CONCLUSIONS

The natural convection of a mass of water contained between two horizontal concentric cylinders has been investigated numerically at temperatures in the neighbourhood of the maximum density. The results obtained in the present study may be summarized as follows:

1) The density inversion has an important effect on natural convection heat transfer in the cavity. This is particularly true in case where two counter eddies of approximately equal size coexist in the gap. For such situations the heat transfer rate is considerably reduced.

2) The presence of a secondary vortex pair, at the top of the inner cylinder, has been found numerically to appear for a very limited temperature range between 6.5^{o} and $7.25^{o}C$, for which the Nusselt number was found to be a minimum. A similar phenomenon has already been observed by Saitoh and Hirose in the case of natural convection around an horizontal ice cylinder.

ACKNOWLEDGEMENT

This work was supported by the National Research Council of Canada through grants NRC A-9201 and NRC A-4197. The authors wish to gratefully thank Ecole Polytechnique for providing necessary time on IBM 360/70.

REFERENCES

1 - POWE, R.E., CARLEY, C.T., and BISHOP, E.H., "Free Convective Flow Patterns in Cylindrical Annuli", Journal of Heat Transfer, Vol. 91, 1969, pp. 210-220.

2 - MACK, L.R., and BISHOP, E.H., "Natural Convection Between Horizontal Concentric Cylinders for Low Rayleigh Numbers", Quarterly Journal of Mechanics and Applied Mathematics, Vol. 21, 1968, pp. 223-241.

3 - KUEHN, T.H., and GOLDSTEIN, R.J., "An Experimental and Theoretical Study on Natural Convection in the Annulus Between Horizontal Concentric Cylinders", Journal of Fluid Mechanics, Vol. 74, 1976, pp. 695-719.

4 - GEBHART, B., and MOLLENDORF, J.C., "Buoyancy-induced Flows in Water under Conditions in which Density Extrema may arise", Journal of Fluid Mechanics, Vol. 89, pp. 673-707.

5 - EDE, A.J., "Heat Transfer by Natural Convection in Refrigerated Liquid", Proc. 8th International Congress Refrigeration, London, 1951, p. 260.

6 - MERK, H.J., "The Influence of Melting and Anomalous Expansion on the Thermal Convection in Laminar Boundary Layers", Applied Science Research, Vol. 4, 1954, pp. 435-452.

7 - DESAI, V.S., and FORBES, R.E., "Free Convection in Water in the Vicinity of Maximum Density, Environmental and Geophysical Heat Transfer, ASME Trans., 1971, pp. 41-47.

8 - WATSON, A., "The Effect of the Inversion Temperature on the Convection of Water in an Enclosed Rectangular Cavity, Quarterly Journal of Mechanics and Applied Mathematics, Vol. 25, 1972, pp. 423-446.

9 - SEKI, N., FUKASAKO, S., and NAKAOKA, M., "Experimental Study on Natural Convection Heat Transfer with Density Inversion of Water Between Two Horizontal Concentric Cylinders", Journal of Heat Transfer, Vol. 97, 1975, pp. 556-561.

10 - FORBES, R.E., and COOPER, J.W., "Natural Convection in a Horizontal Layer of Water Cooled from about to near Freezing", Journal of Heat Transfer Vol. 97, 1975, pp. 47-53.

11 - VASSEUR, P., and ROBILLARD, L., "Transient Natural Convection Heat Transfer in a Mass of Water Cooled Through 4°C, International Journal of Heat and Mass Transfer, Vol. 23, pp. 1195-1205.

12 - CHENK, K.C., and TAKEUCHI, M., "Transient Natural Convection of Water in a Horizontal pipe with Constant Cooling Rate through 4°C", Journal of Heat Transfer, Vol. 98, 1976, pp. 581-587.

13 - ROBILLARD, L., and VASSEUR, P., "Transient Natural Convection Heat Transfer of Water with Maximum Density Effect and Super Cooling", National Heat Transfer Conference, Orlando, Florida, 1980, ASME Paper No. 80-HT-74.

14 - GRAY, D.D., and GIORGINI, A., "The Validity of the Boussinesq Approximation for Liquids and Gases", International Journal of Heat and Mass Transfer, Vol. 19, 1976, pp. 545-551.

15 - CHANDRASEKHAR, S., "Hydrodynamic and Hydromagnetic Stability", Oxford University Press.

16 - FUJII, T., "Fundamentals of Free Convection Heat Transfer", Progress in Heat Transfer Engineering, Vol. 3, 1974, pp. 66-67.

17 - LANDOLT-FORNSTEIN, ZAHLENWERTE UND FUNKTIONEN, Springer-Verlag II (1), 1971, pp. 36-37.

18 - MALLISON, G.D., and DE VAHL DAVIS, D., "The Method of the False Transient for the Solution of Coupled Elliptic Equations", Journal of Computational Physics, Vol. 12, 1973, pp. 435-461.

19 - ROACHE, P., "Computational Fluid Dynamics", Hermosa Publishers, 1976.

20 - GRAWFORD, L., and LEMLICH, R., "Natural Convection in Horizontal Concentric Cylindrical Annuli", IEC Fundamentals 1, 1962, pp. 260-264.

21 - CHARRIER-MOJTABI, M.C., MOJTABI, A., and CALTAGIRONE, J.P., "Numerical Solution of a Flow due to a Natural Convection in Horizontal Cylindrical Annulus", Vol. 101, 1979, pp. 171-173.

22 - BISHOP, E.H., and CARELY, C.T., "Photographic Studies of Natural Convection between Concentric Cylinders", Proceedings Heat Transfer Fluid Mechanics Institute, 1966, pp. 63-78.

23 - SAITOH, T., and HIROSE, K., "Thermal instability of Natural Convection Flow over a Horizontal Ice Cylinder Encompassing a Maximum Density Point", Journal of Heat Transfer, Vol. 102, 1980, pp. 261-267.

24 - ROBILLARD, L., and VASSEUR, P., "Effect du maximum de densité sur la convection libre de l'eau dans une cavité fermée", Canadian Journal of Civil Engineering, Vol.6, 1979, pp. 481-493.

LIST OF FIGURES

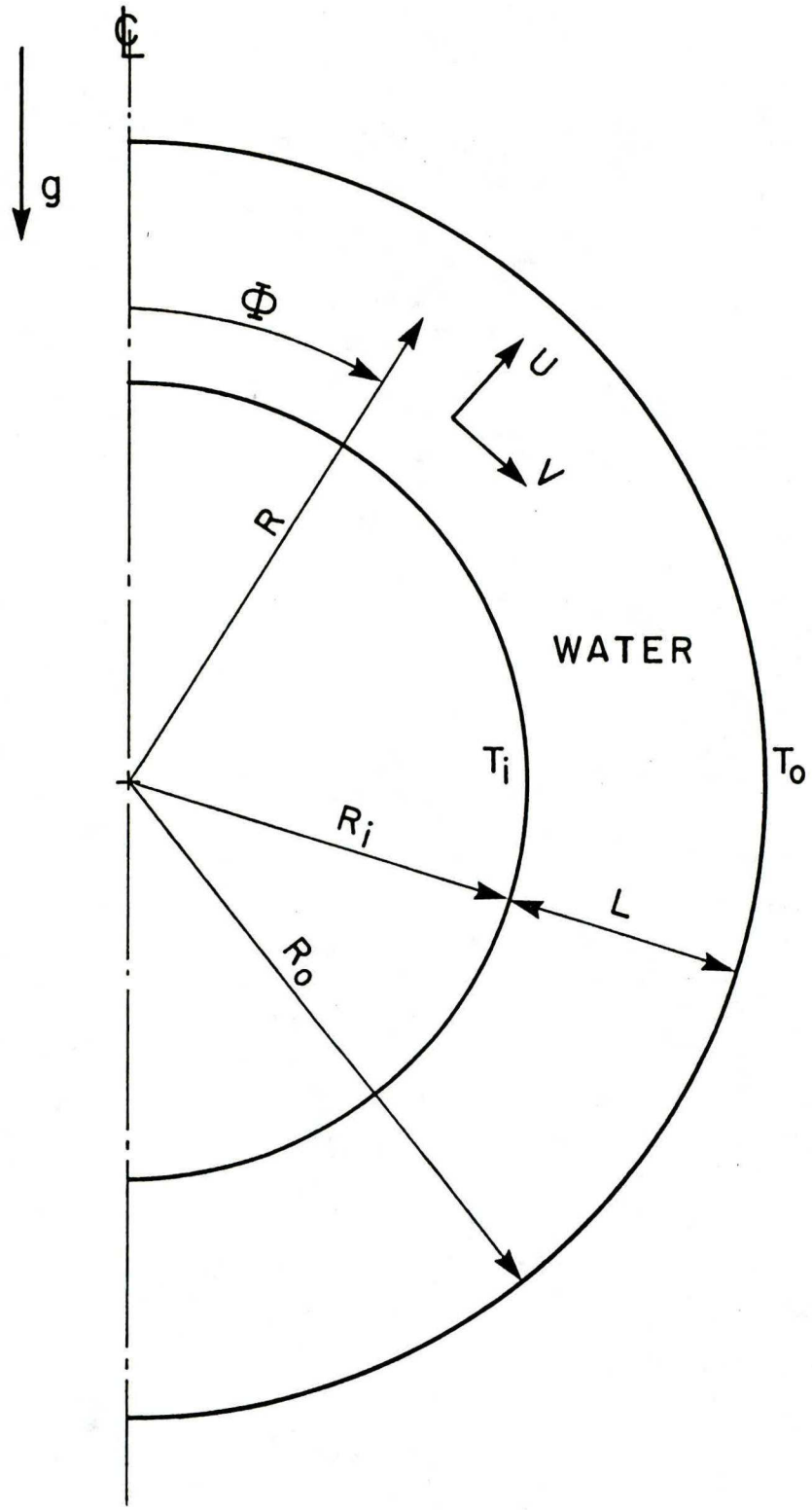

Fig. 1: Flow geometry and coordinate system.

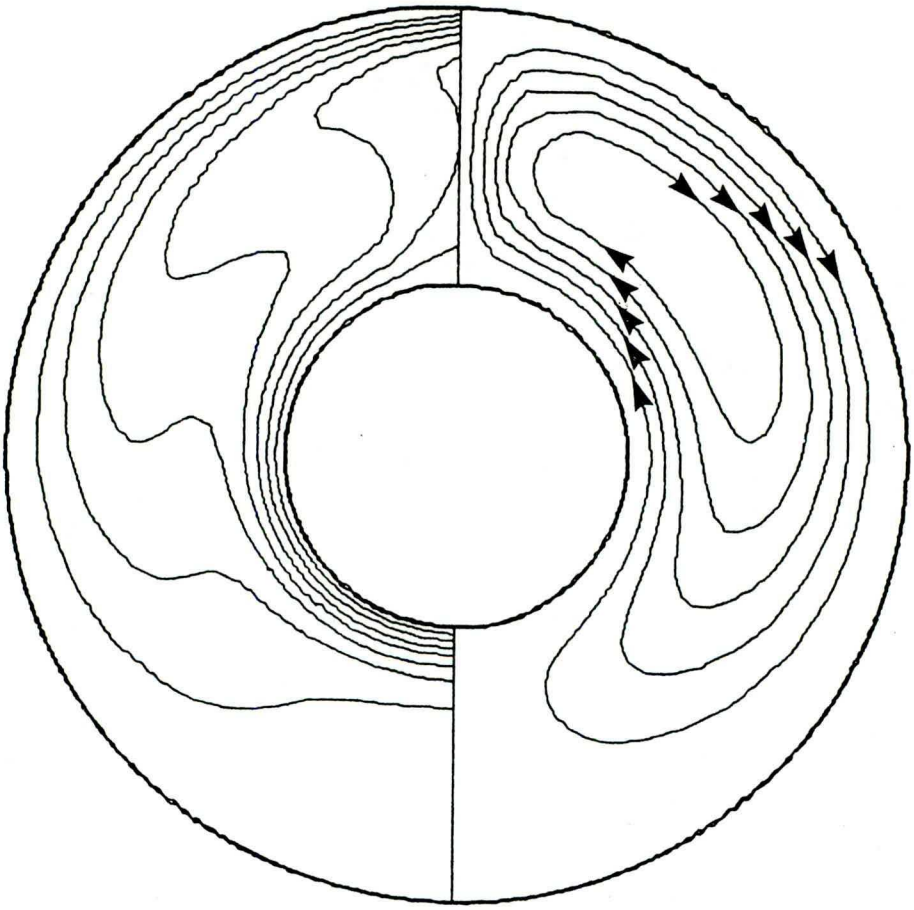

Fig. 2: Isotherms and streamlines for $A = 2.2 \times 10^9$, $B = 0.8$, $T_i = 0^{\circ}C$ and $T_o = 4^{\circ}C$.

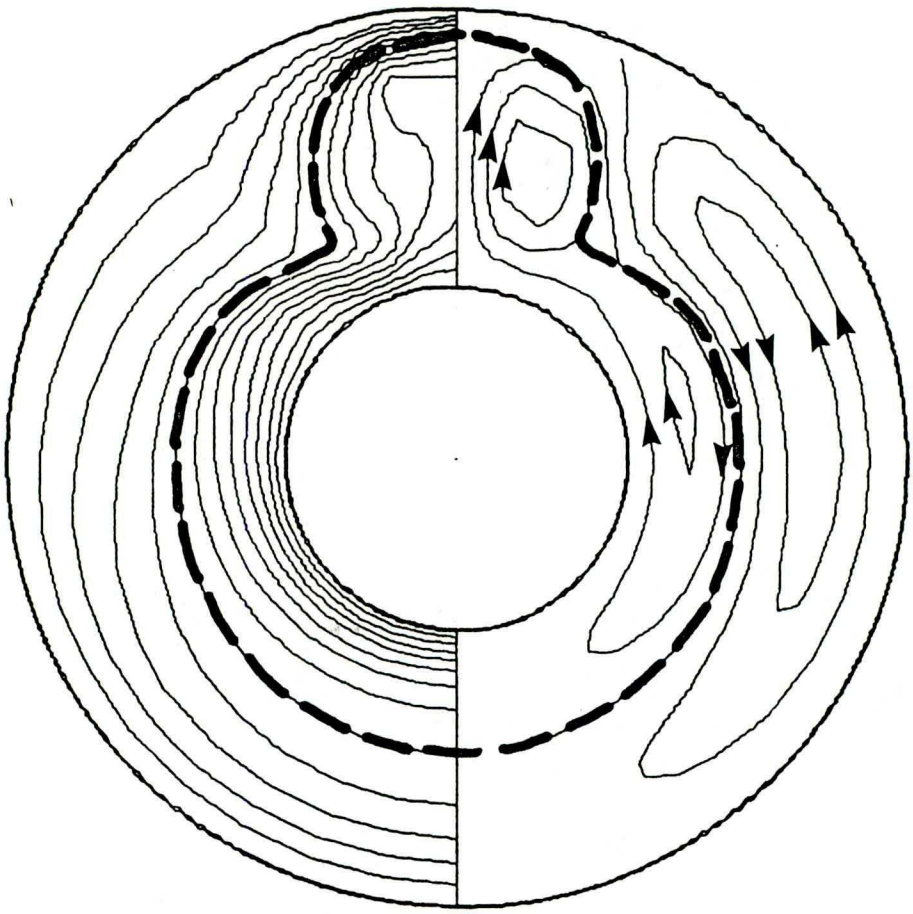

Fig. 3: Isotherms and streamlines for $A = 2.2 \times 10^9$, $B = 0.8$, $T_i = 0^{\circ}C$ and $T_o = 6.5^{\circ}C$.

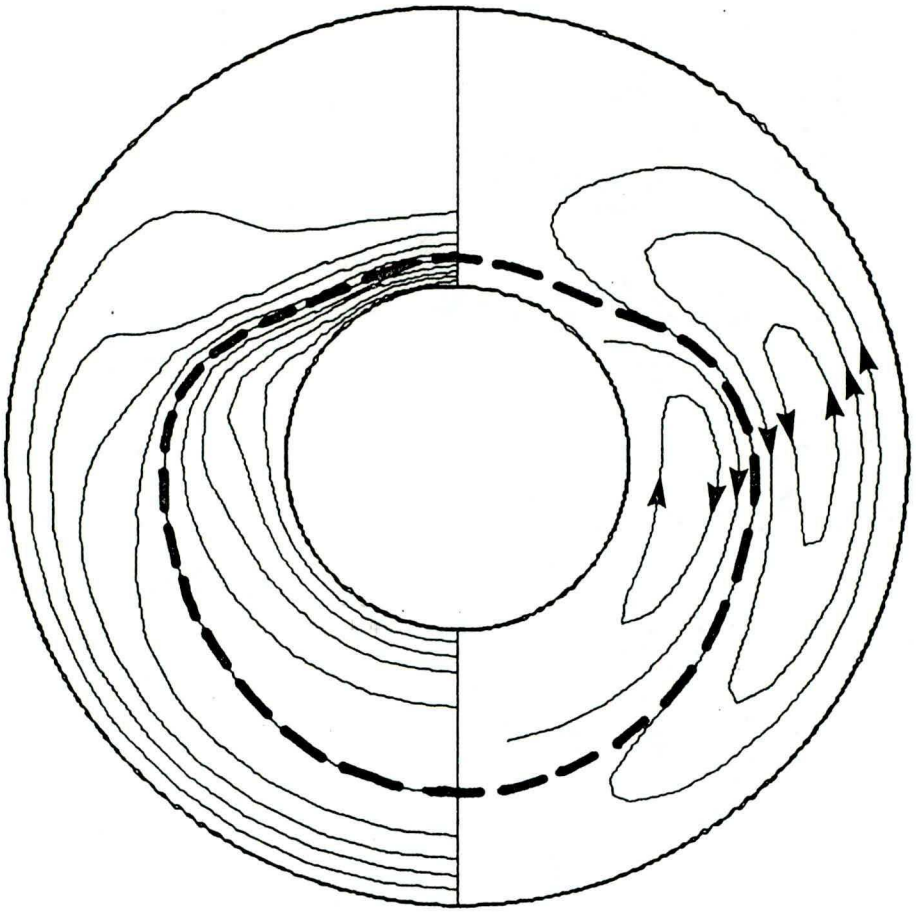

Fig. 4: Isotherms and streamlines for $A = 2.2 \times 10^9$, $B = 0.8$, $T_i = 0^{\circ}C$ and $T_o = 8^{\circ}C$.

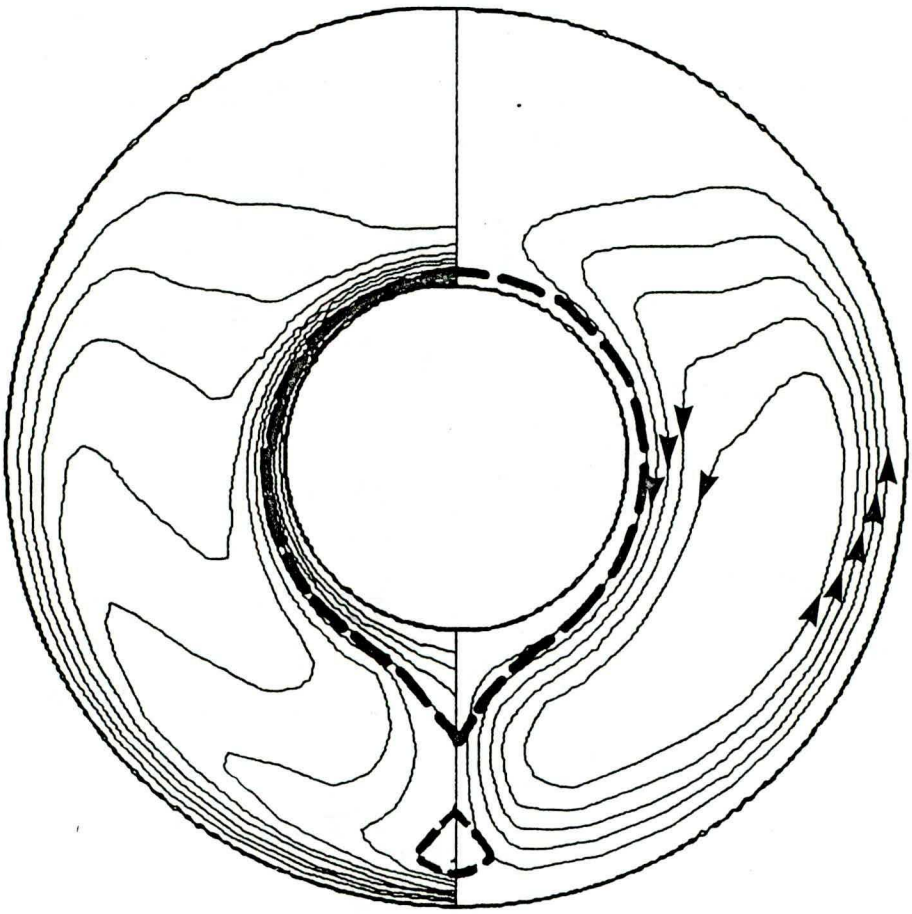

Fig. 5: Isotherms and streamlines for $A = 2.2 \times 10^9$, $B = 0.8$, $T_i = 0^oC$ and $T_o = 12^oC$.

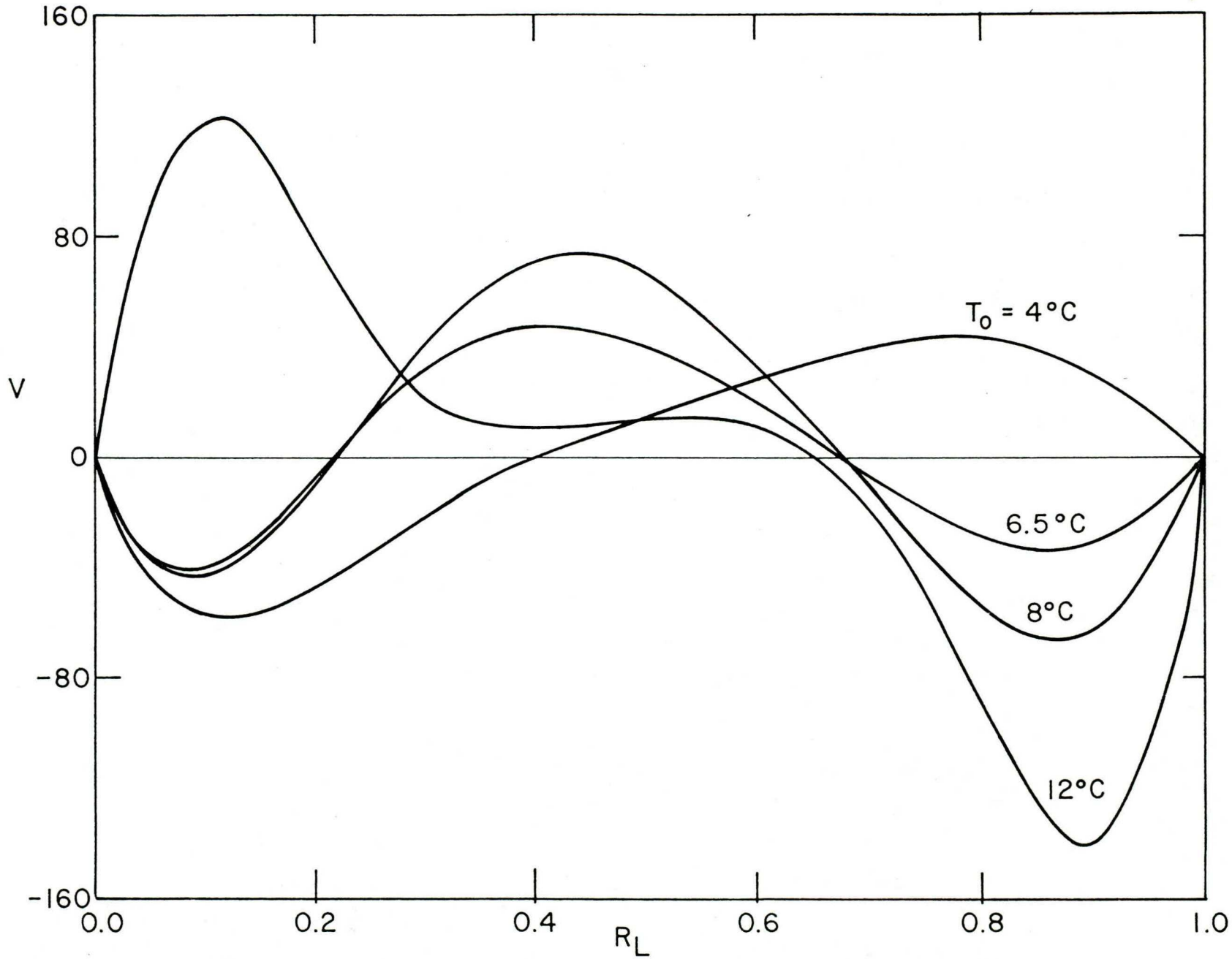

Fig. 6: Angular velocity profile at $\Phi = 90^{o}C$ for $A = 2.2 \times 10^{9}$, $B = 0.8$, $T_i = 0^{o}C$ and different values of T_o.

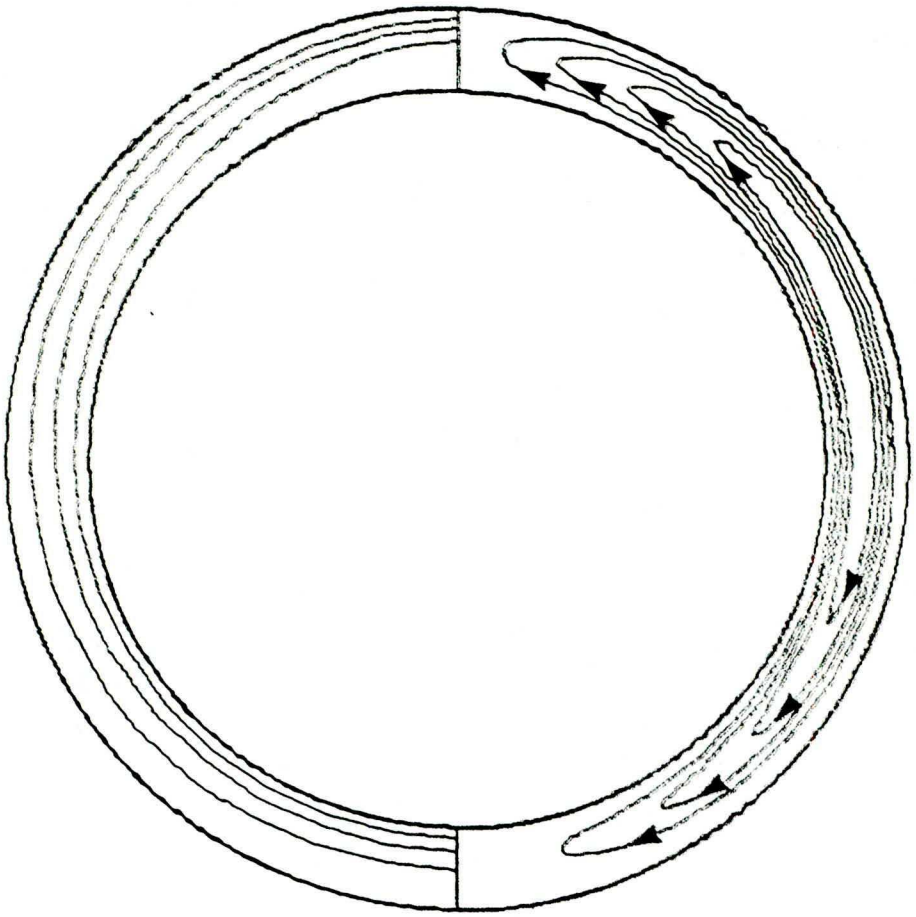

Fig. 7: Isotherms and streamlines for $A = 7.0 \times 10^8$, $B = 0.11$, $T_i = 0^oC$ and $T_o = 4^oC$.

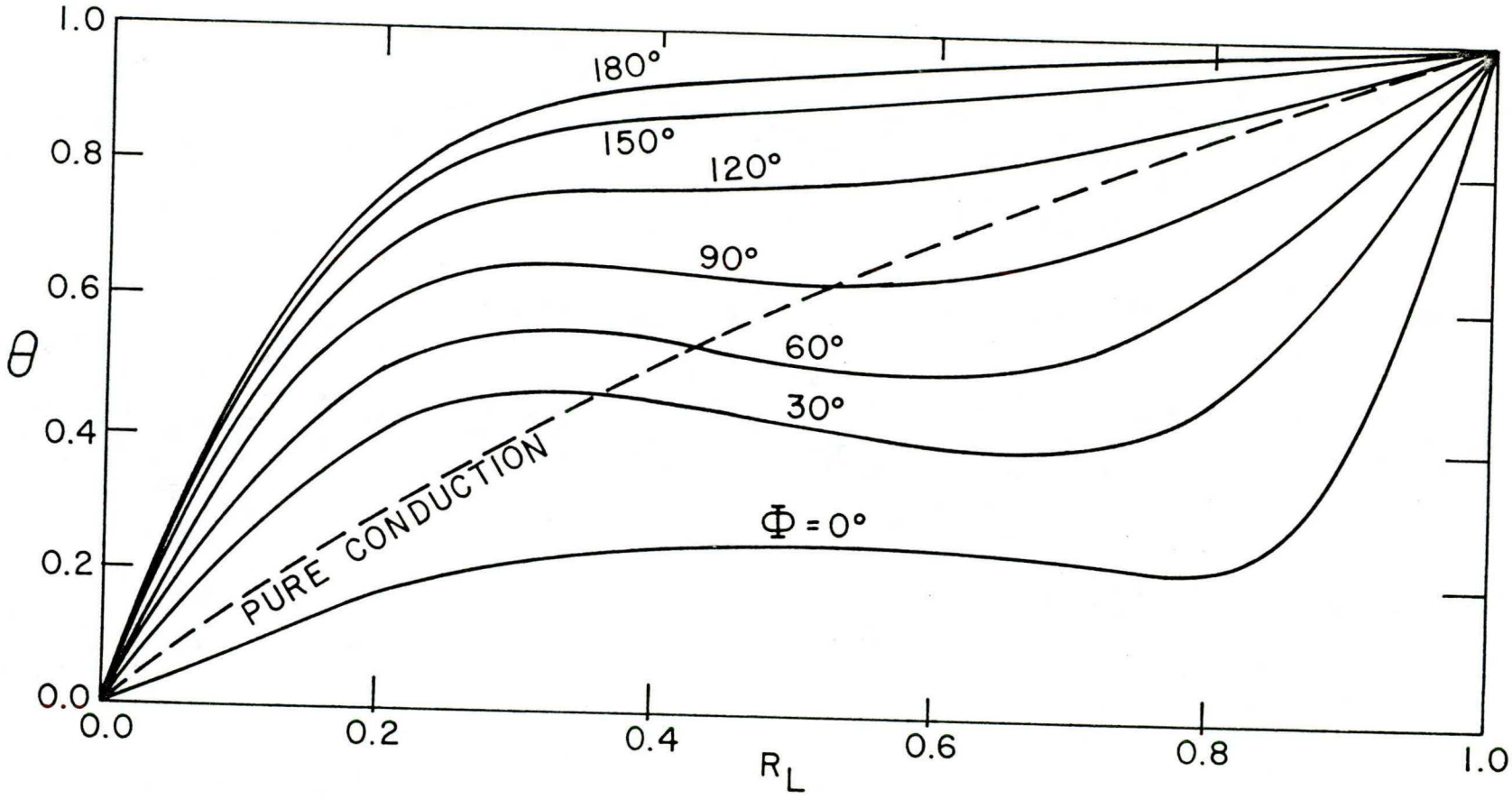

Fig. 8(a) Temperature profile for A = 2.2 x 10^9, B = 0.8, $T_i = 0^oC$ and $T_o = 4^oC$.

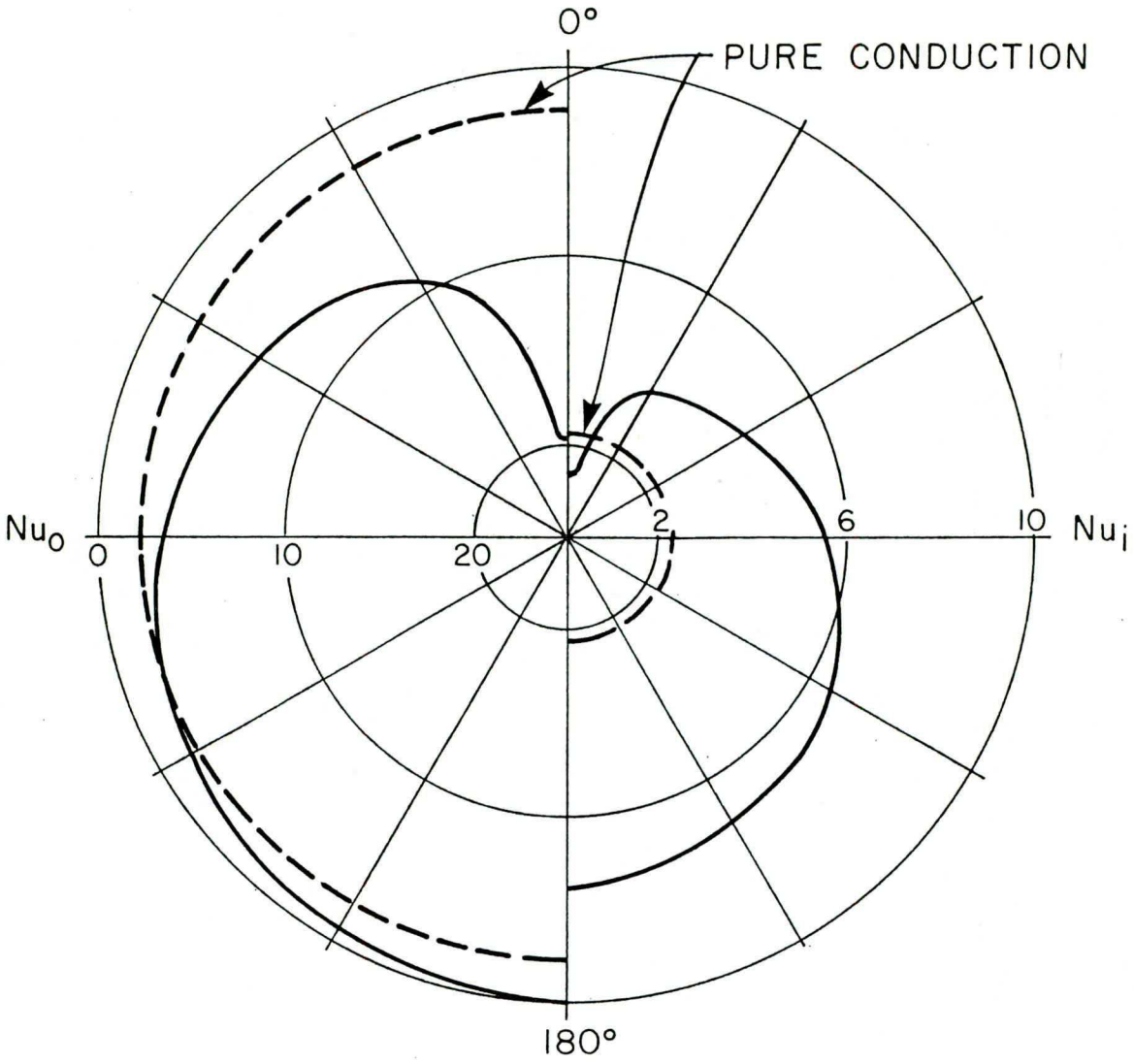

Fig. 8(b) Distribution of local Nusselt number for $A = 2.2 \times 10^9$, $B = 0.8$, $T_i = 0^\circ C$ and $T_o = 4^\circ C$.

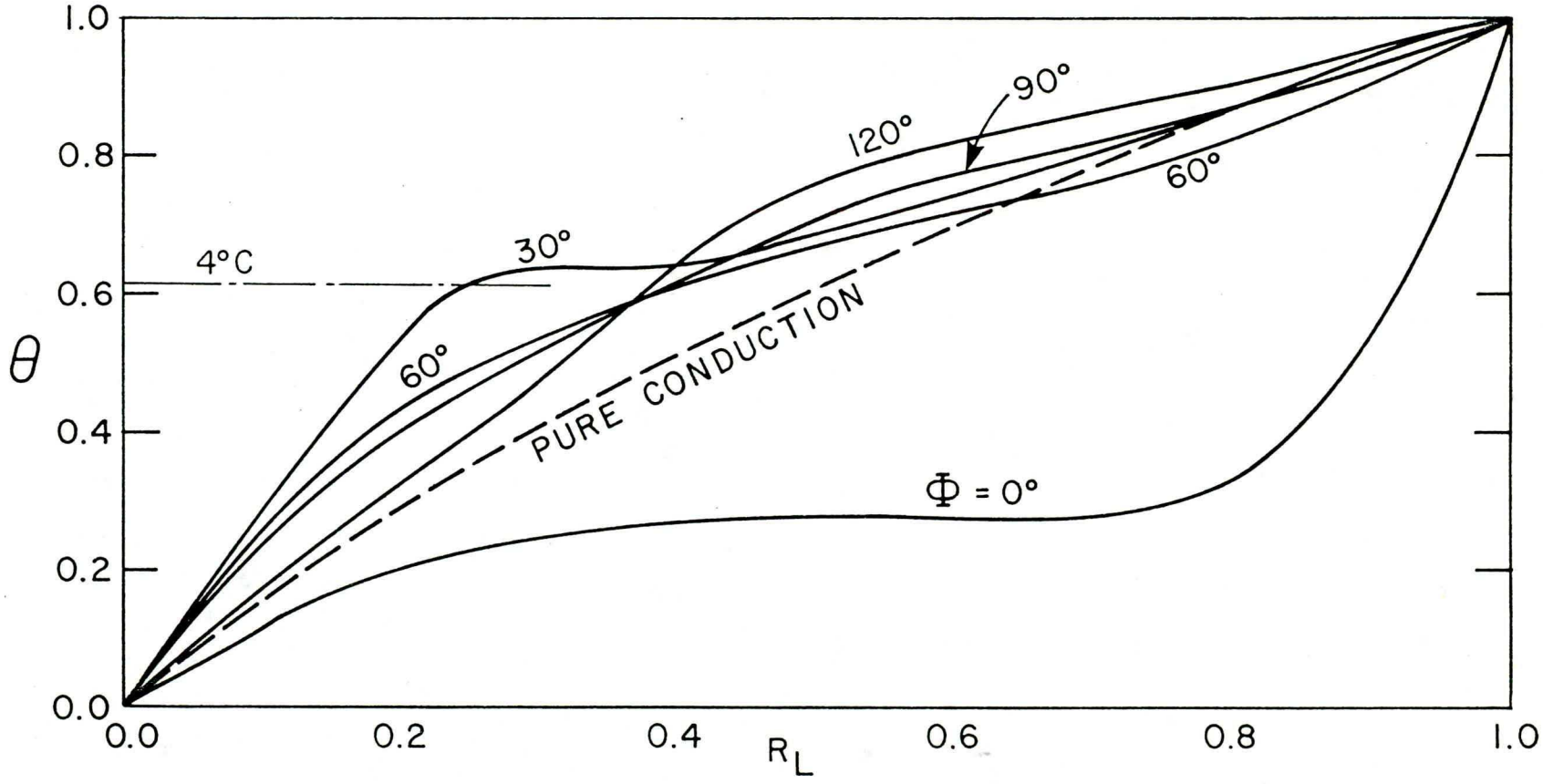

Fig. 9(a): Temperature profile for A = 2.2×10^9, B = 0.8, $T_i = 0^oC$ and $T_o = 6.5^oC$.

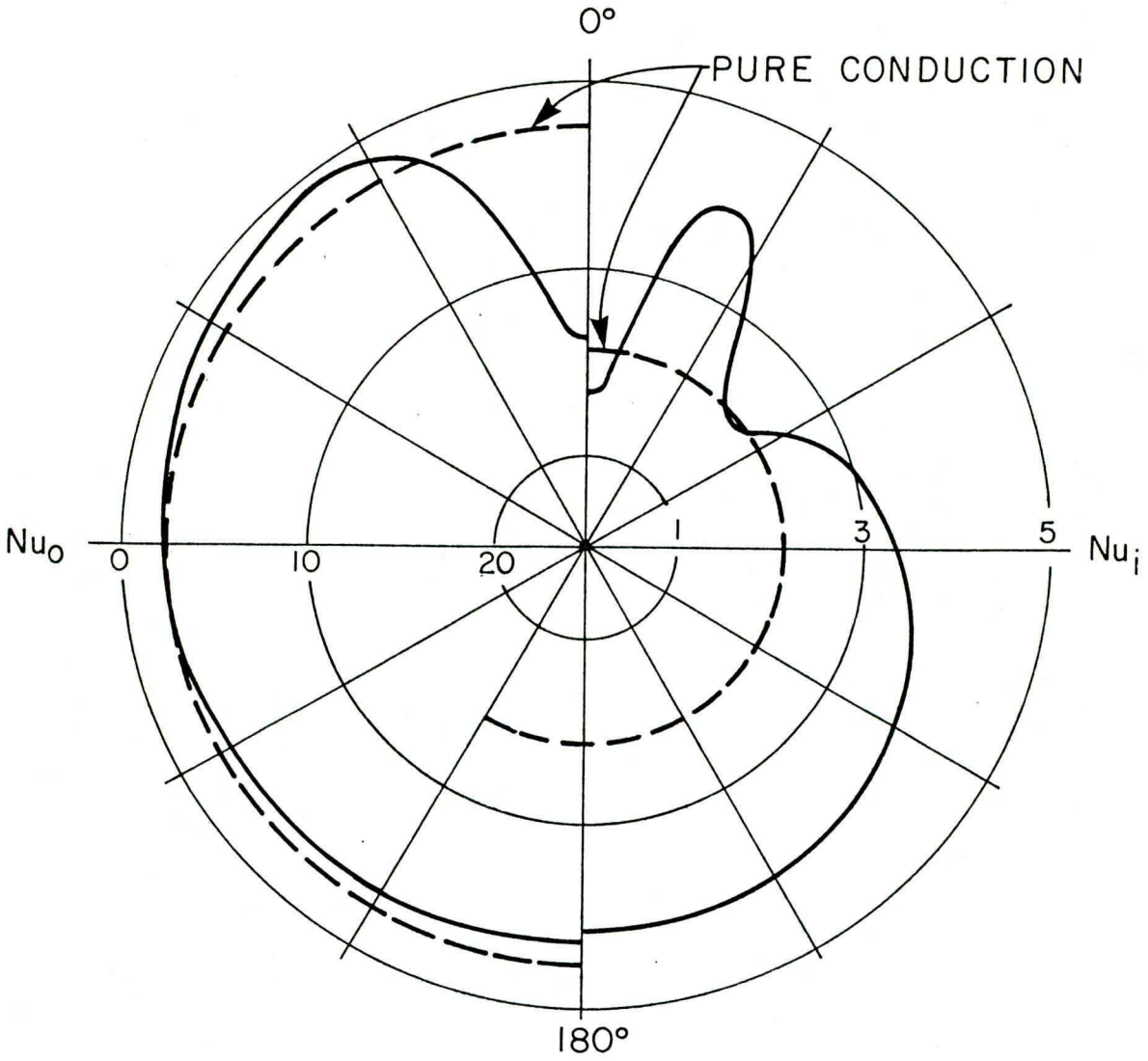

Fig. 9(b): Distribution of local Nusselt number for $A = 2.2 \times 10^9$, $B = 0.8$, $T_i = 0^oC$ and $T_o = 6.5^oC$.

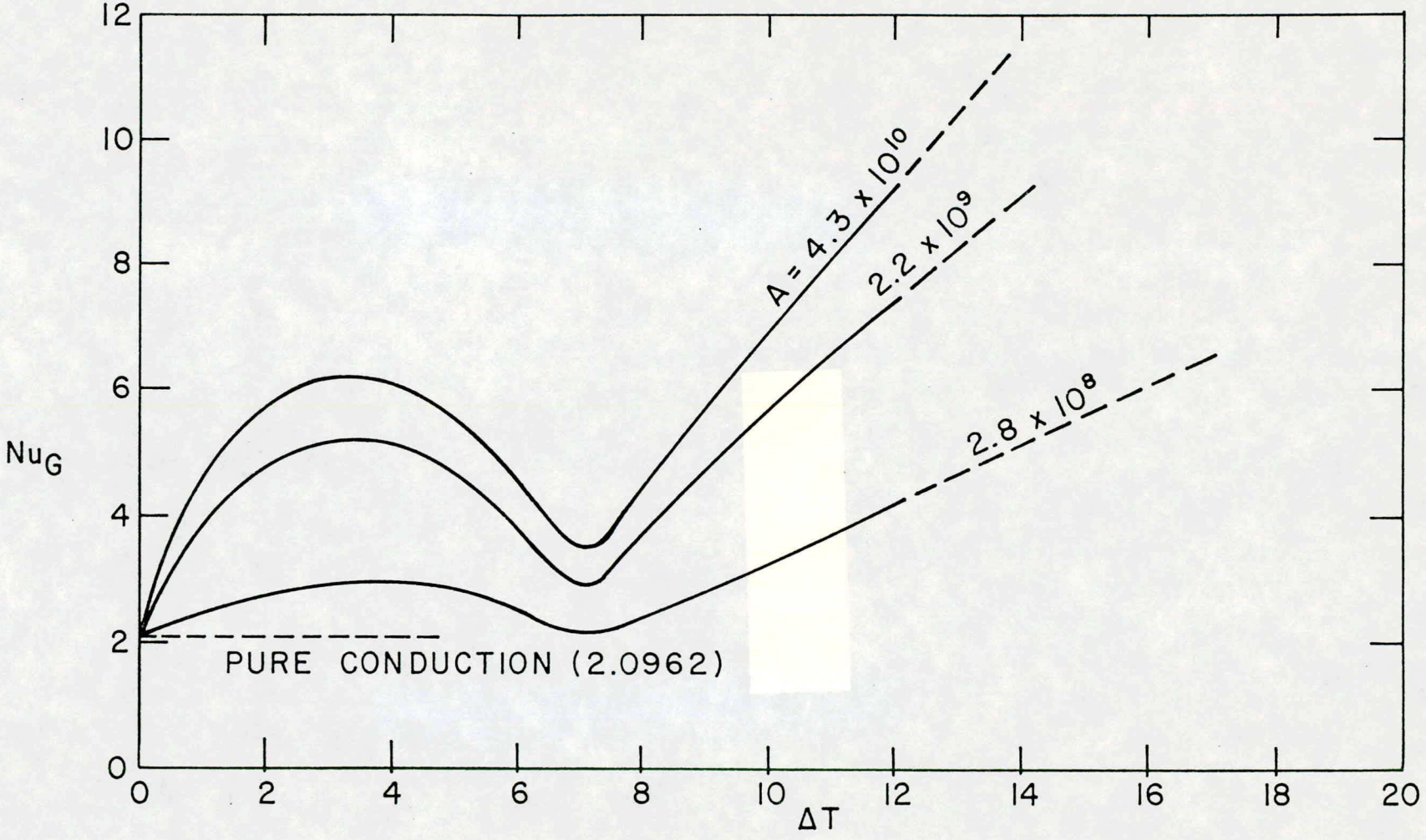

Fig. 10 Global Nusselt number Nu_G as a function of ΔT for various values of A.